2010

Islands and holes as measures of mass balance in growth of the $(\sqrt{3}\times\sqrt{3})R30°$ phase of Ag on Si(111)

Alex Belianinov
Iowa State University

Barış Ünal
Iowa State University

Ning Lu
Iowa State University

Min Ji
Iowa State University

Kai-Ming Ho
Iowa State University, kmh@ameslab.gov
See next page for additional authors

Islands and holes as measures of mass balance in growth of the $(\sqrt{3}\times\sqrt{3})R30°$ phase of Ag on Si(111)

Abstract
It is well known that conversion of Si(111)-(7×7) into the $(\sqrt{3}\times\sqrt{3})R30°$ phase of adsorbed Ag requires a change in the Si density, and causes formation of islands and holes at the surface. By mass balance, the ratio of areas of islands and holes (R_{IH}) should be approximately 1. However, we find that the ratio is significantly higher, depending on preparation conditions. A possible explanation would be that there are different types of $(\sqrt{3}\times\sqrt{3})R30°$ structures. However, neither scanning tunneling microscopy nor density-functional theory (implemented as a genetic algorithm search) supports this explanation. We propose that the edges of the islands contain excess Ag which becomes available to expand the holes, when the island perimeter decreases. Under certain conditions, excess Ag is also made available by dissolution of small islands that are Ag rich.

Keywords
Ames Laboratory, Materials Science and Engineering, Physics and Astronomy

Disciplines
Biological and Chemical Physics | Materials Science and Engineering | Physical Chemistry

Comments
This article is from *Physical Review B* 82, no. 24 (2010): 245413, doi:10.1103/PhysRevB.82.245413.

Authors
Alex Belianinov, Barış Ünal, Ning Lu, Min Ji, Kai-Ming Ho, Cai-Zhuang Wang, Michael C. Tringides, and Patricia A. Thiel

Islands and holes as measures of mass balance in growth of the $(\sqrt{3}\times\sqrt{3})R30°$ phase of Ag on Si(111)

Alex Belianinov,[1,2] Barış Ünal,[1,3,*] Ning Lu,[1,4] Min Ji,[1,4] K.-M. Ho,[1,4] C.-Z. Wang,[1,4] M. C. Tringides,[1,4] and P. A. Thiel[1,2,3]
[1]*Ames Laboratory, Iowa State University, Ames, Iowa 50011, USA*
[2]*Department of Chemistry, Iowa State University, Ames, Iowa 50011, USA*
[3]*Department of Materials Science and Engineering, Iowa State University, Ames, Iowa 50011, USA*
[4]*Department of Physics and Astronomy, Iowa State University, Ames, Iowa 50011, USA*
(Received 30 March 2010; revised manuscript received 8 October 2010; published 10 December 2010)

It is well known that conversion of Si(111)-(7×7) into the $(\sqrt{3}\times\sqrt{3})R30°$ phase of adsorbed Ag requires a change in the Si density, and causes formation of islands and holes at the surface. By mass balance, the ratio of areas of islands and holes (R_{IH}) should be approximately 1. However, we find that the ratio is significantly higher, depending on preparation conditions. A possible explanation would be that there are different types of $(\sqrt{3}\times\sqrt{3})R30°$ structures. However, neither scanning tunneling microscopy nor density-functional theory (implemented as a genetic algorithm search) supports this explanation. We propose that the edges of the islands contain excess Ag which becomes available to expand the holes, when the island perimeter decreases. Under certain conditions, excess Ag is also made available by dissolution of small islands that are Ag rich.

DOI: 10.1103/PhysRevB.82.245413 PACS number(s): 68.37.Ef, 68.55.−a, 81.15.Aa, 68.47.Fg

I. INTRODUCTION

Reconstructive transitions at surfaces, i.e., transitions that require a change in surface atomic density, have long been a subject of investigation in surface science. Before the advent of scanning tunneling microscopy (STM), the reservoir that supplied or consumed the "extra" surface atoms was debated. One example was the adsorbate-induced (1×2)-to-(1×1) transition of Pt(110), where the data showed that a half monolayer (ML) of Pt atoms rearrange by moving over only a few lattice constants, and models were created or rejected accordingly.[1,2] With STM, it was discovered that atoms produced in such a structural transition simply form new islands on terraces.[3] Investigations of mass balance in systems such as this can lead to other important results, such as differentiation between proposed structural models.[4]

The conversion of the Si(111) surface from the (7×7) phase to a $(\sqrt{3}\times\sqrt{3})R30°$ surface phase is one such transition. This conversion requires adsorption of Ag, and temperatures in the range of about 500–900 K.[5] When the (7×7) converts to the $(\sqrt{3}\times\sqrt{3})R30°$—called $\sqrt{3}$ herein—the change in Si density causes the $\sqrt{3}$ to partition locally into regions above the (7×7), i.e., "islands," and regions below the (7×7), i.e., "holes."[6–11] (This assumes little or no participation by step edges, which is valid if terraces are sufficiently wide or temperatures low.[11]) The hole and island features are illustrated schematically in Fig. 1(a), and by experimental data in Fig. 1(b). A similar partitioning occurs during development of the $\sqrt{3}$ structure of Au on Si(111).[8,12]

Because of Si mass balance, the areal ratio of islands to holes (R_{IH}) can be, and has been, used to deduce the density of Si in the $\sqrt{3}$ phase. (See the Appendix.) Using STM, both Shibata *et al.*[8,9] and Wan *et al.*[10] measured $R_{IH}\approx1$ and deduced the density to be 1 Si atom per (1×1) unit-cell area, i.e., 1 ML. This means that half of the Si bilayer [plus the adatoms of the (7×7)] are missing in the $\sqrt{3}$ relative to the unreconstructed Si surface, as shown in Fig. 1(a).

These results helped to shape and support the current model for the $\sqrt{3}$. This model is known as the inequivalent triangle (IET) model,[13,14] and it can be viewed as an asymmetrical variation in the well-known honeycomb chain trimer (HCT) model.[15]

However, the issue of mass balance in this system is not settled. Previously, McComb *et al.*[11] reported that R_{IH} can exceed its ideal value by almost a factor of 2, and that R_{IH}

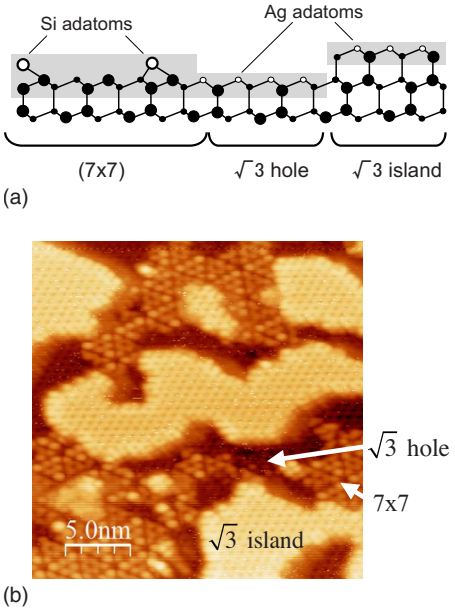

FIG. 1. (Color online) (a) Schematic of the Si(111) surface, illustrating the formation of $\sqrt{3}$ islands and holes from the (7×7), modeled after Fig. 5 of Ref. 9. The shaded regions represent the depth over which atoms are counted for calculating atom densities in the Appendix, after Refs. 9 and 10. Small open circles are Ag atoms, large white circles are Si adatoms in the (7×7), and black circles are other Si atoms. (b) STM image illustrating $\sqrt{3}$ islands, $\sqrt{3}$ holes, and (7×7) phase. The surface was prepared by depositing 0.69 ML Ag at 615 K and then annealing for 2 min. Image size is 25×25 nm^2. Tunneling conditions are bias voltage (V_T)=−1.0 V and tunneling current (I_T)=0.2 nA.

varies with Ag coverage, for deposition temperature of 720 K. At low Ag coverage, they attributed the deviation to participation of pre-existing Si steps, but at higher coverage the reason for $R_{IH}>1$ was unclear. On the other hand, Wan *et al.*[10] reported that R_{IH} is independent of Ag coverage, at an unspecified deposition temperature. This leads to the question of whether R_{IH} is sensitive to preparation conditions and, if so, why? There has been no report of how R_{IH} depends on thermal history, aside from a brief remark in one paper that R_{IH} is not sensitive to substrate temperature.[10]

In this paper, we find that the value is very sensitive to deposition temperature and/or annealing time. To understand the thermal evolution of R_{IH} we will draw upon previous, extensive investigations into evolution of the $\sqrt{3}$ phase[6–11,16–18] but a new element must be introduced as well. We will propose that the edges of the $\sqrt{3}$ islands contain Ag at a concentration above (and Si below) that of the ideal $\sqrt{3}$. As deposition temperature or annealing time increases, the $\sqrt{3}$ islands become larger and more compact. Hence, the total island perimeter decreases, which drives R_{IH} toward its ideal value.

II. EXPERIMENTAL AND COMPUTATIONAL DETAILS

The experimental ultrahigh vacuum system, including the variable-temperature STM and Ag evaporator, are described elsewhere.[19] The Si sample is *p*-type with resistivity of 0.02 Ω cm. Ag flux is typically 0.1–0.2 ML/min. Ag is deposited or annealed at elevated temperature, then cooled to room temperature for STM imaging in constant-current mode. Ag coverage is determined as follows. We assume that local Ag coverage in the islands and holes is 1 ML when $R_{IH}=1$. Then the total Ag coverage is calculated as the combined area of islands and holes, divided by the total surface area when $R_{IH}=1$. Silver coverage is assumed constant throughout an individual experiment (no loss of Ag due to evaporation or subsurface migration). R_{IH} is extracted from STM data by setting a height cutoff and summing the area (number of pixels) above or below this cutoff.[20] Images are examined carefully to make sure that cutoffs are physically reasonable.

Some groups report that structures with IET symmetry transform reversibly to apparent HCT symmetry around 300 K, due to thermal fluctuations in the IET structure.[21–23] However, Zhang *et al.* report that the IET structure can exist statically even at room temperature.[24,25] In the present work, we observe only the apparent HCT structure.

In the computations, we implement a variable-number genetic algorithm (GA) search in which both the number of Ag and Si atoms are variable. The structures in each generation are relaxed using density-functional theory (DFT). The calculations are carried out within the local-density approximation of DFT (Refs. 26 and 27) using projector-augmented-wave potentials,[28] as implemented in the Vienna *ab initio* simulation package.[29] The kinetic-energy cutoff is set to 250 eV and the 4×4 Monkhorst-Pack grid is used for the surface Brillouin zone. The system is modeled as a periodically repeating slab consisting of: two fixed Si bilayers, the bottom one hydrogen passivated; a reconstructed Ag/Si layer on the top; and a vacuum gap of ~0.8 nm. All the models are based on a $(\sqrt{3}\times\sqrt{3})R30°$ surface unit cell, using a Si bulk lattice constant of 0.540 nm. The two Si bilayers are fixed at the bulk crystalline positions, and the Si-H distance is fixed at 0.151 nm. The remaining Ag and Si atoms are relaxed until the residual force is smaller than 0.25 eV/nm.

The formation energy, E_f [per (1×1) unit cell] is calculated from $E_f=(1/3)(E_{tot}-E_{sub})-N_{Si}\times\mu_{Si}-N_{Ag}\times\mu_{Ag}$, where E_{tot} is the total energy and E_{sub} is the energy of the subsurface region (two Si bilayers and one layer of hydrogen). The μ_{Si} and μ_{Ag} are chemical potentials of Si and Ag bulk phases, respectively, while $N_{Si,\sqrt{3}}$ and $N_{Ag,\sqrt{3}}$ are the number of Si and Ag atoms in the surface layer per (1×1) unit cell (identical to coverages in ML) on top of the fixed substrate. See also the Appendix and Fig. 1.

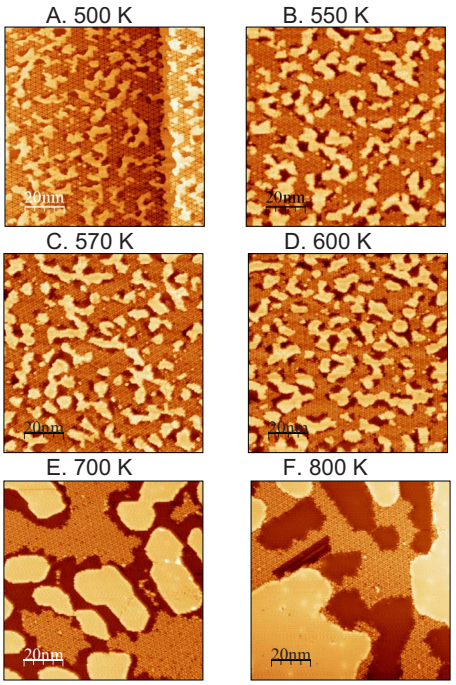

FIG. 2. (Color online) STM images after Ag deposition at various temperatures. All images are 100×100 nm^2. Unless noted otherwise, $V_T=-1.0$ V and $I_T=0.2$ nA. Values of R_{IH} are averages over multiple images. (a) $T_{dep}=500$ K, 0.49 ML Ag, $R_{IH}=5.4$. (b) $T_{dep}=550$ K, 0.46 ML Ag, $R_{IH}=3.8$. (c) $T_{dep}=570$ K, 0.44 ML Ag, $R_{IH}=3.5$. (d) $T_{dep}=600$ K, 0.53 ML Ag, $R_{IH}=3.0$. (e) $T_{dep}=700$ K, 0.73 ML Ag, $R_{IH}=1.7$, $V_T=-2.0$ V, $I_T=0.5$ nA. (f) $T_{dep}=800$ K, 0.53 ML Ag, $R_{IH}=1.0$, $V_T=-1.0$ V, $I_T=2$ nA.

III. EXPERIMENTAL RESULTS AND INTERPRETATION

A. Changes in R_{IH}

In our STM experiments, residual (7×7) always coexists with islands and holes because the Ag coverage is deliberately adjusted to be in the submonolayer range, i.e., insufficient for complete conversion of the (7×7). The two parameters that we vary systematically are (i) the temperature at which Ag is deposited, T_{dep}; and (ii) the time, t_{ann}, of annealing after deposition ends. Focusing first on the deposition temperature, Fig. 2 is a series of STM images after deposi-

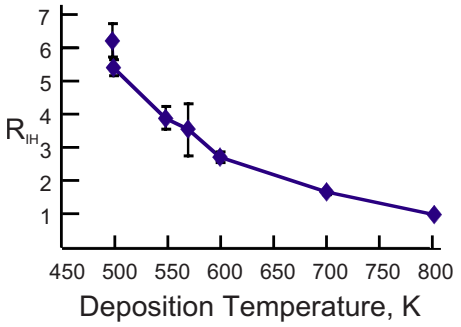

FIG. 3. (Color online) R_{IH} as a function of deposition temperature. The sample was held for 1 min at T_{dep} after deposition finished, with the exception of the first point. There, $R_{IH}=6.2$ at 500 K, and the ratio was measured immediately after deposition. Values are averages over multiple images, and error bars are standard deviations. If no error bars are visible, they are obscured by the symbol.

tion of 0.4–0.6 ML Ag at varying temperatures, followed by annealing for 1–2 min. The fractional area of 7×7 that remains unconverted ranges from 0.6 to 0.4 in these experiments. We count the elevated regions as islands, regardless of the structure (or lack thereof) on top of the island. The dark areas—holes—are so small that they are barely evident in Fig. 2(a) but they become larger as T_{dep} increases.

Figure 3 shows R_{IH} over the same range of T_{dep} as in Fig. 2. R_{IH} is as high as 6 after Ag deposition at 500 K. It falls to $R_{IH}\approx1$ at $T_{dep}=800$ K. Postdeposition annealing experiments show the same trend as a function of time. Figure 4(a) shows a case where R_{IH} falls from an initial value of 2.7, and approaches 1 at long t_{ann}, following deposition at 600 K. From both the deposition and annealing experiments, we conclude that $T_{dep}<800$ K can easily lead to $R_{IH}>1$ but $R_{IH}\approx1$ is the limiting value.

Shibata *et al.*[6,7] have reported that Ag nucleates into islands that serve as precursors to the $\sqrt{3}$. From data taken with *in situ* STM, and working at temperatures of ~440–525 K, they concluded that these Ag islands can convert to $\sqrt{3}$, but only if they are above a critical size of two 7×7 unit cells (about 12 nm^2). We therefore considered the possibility that small islands are Ag rich, and that they can provide the Ag needed for expansion of the holes. If this were the case, then by stoichiometry only half of the excess Ag (the amount in excess of the 1:1 Ag:Si stoichiometry of the ideal $\sqrt{3}$) in the small islands could go toward hole expansion; the other half would need to join existing large islands, in order to consume Si ejected from the surface. The total island area and the hole area would increase by equal amounts, but simple arithmetic shows that R_{IH} would still decrease if its initial value exceeds 1.

Indeed, small islands are evident in the STM images [see Figs. 2(a)–2(d)], and they disappear during annealing. In our experiments, the lower limit of stability is about 50 nm^2 rather than 12 nm^2, perhaps because the temperature is somewhat higher than that used by Shibata *et al.* Figure 4(b) shows the number density of islands below and above 50 nm^2 during annealing at 600 K. Most small islands disappear within the first 20 min. In the same period, the change in R_{IH} is 40% of the total change that occurs by the end of

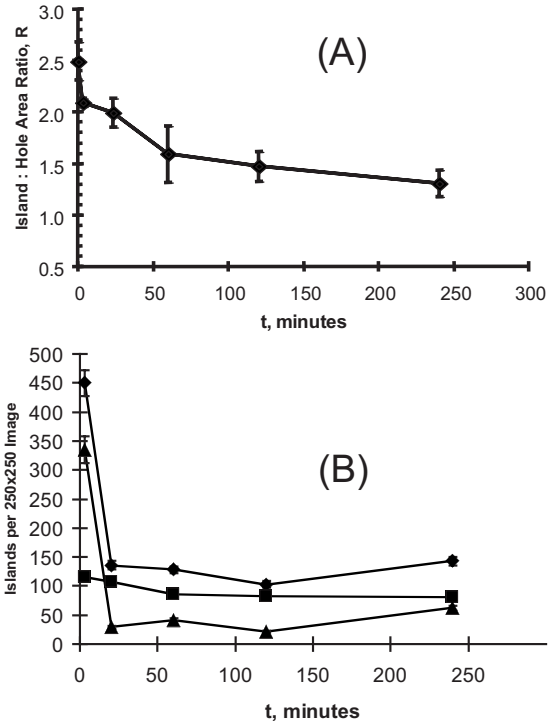

FIG. 4. (a) R_{IH} as a function of t_{ann} at 600 K. At $t_{ann}=0$, deposition has just ended. Values are averages over multiple images, and error bars are standard deviations over images within a single run. (b) Densities of islands as a function of t_{ann} at 600 K. The diamonds show all islands, triangles show islands with individual areas ≤50 nm^2, and squares show larger islands. Error bars show the standard deviation of the island density in various images. Images are weighted according to their size. When error bars are not visible, they are covered by the individual data point.

the experiment. We conclude that the small islands do contribute some of the mass needed to reduce R_{IH}, but not all.

More information comes from examining the evolution of areas (A) of the islands, holes, and (7×7) matrix. Figure 5 shows these data for an experiment in which the surface is annealed at 600 K, starting from an initial value of $R_{IH}=2.7$ [cf. Fig. 4(a)]. In the first 30 min, there is an initial

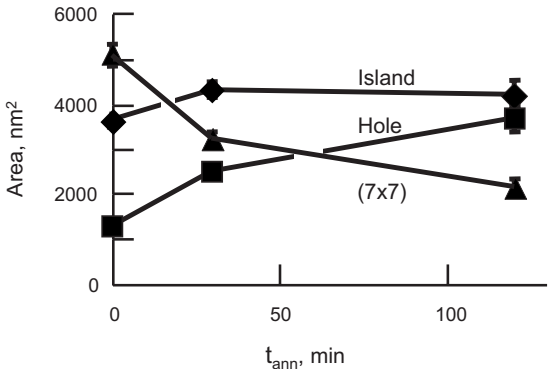

FIG. 5. Graph illustrating the change in areas of Si(111)-7×7 phase (triangles), $\sqrt{3}$ islands (diamonds) and $\sqrt{3}$ holes (circles) with annealing time at 600 K. Values are averages over multiple images and error bars are standard deviations. Most error bars are obscured by the symbols.

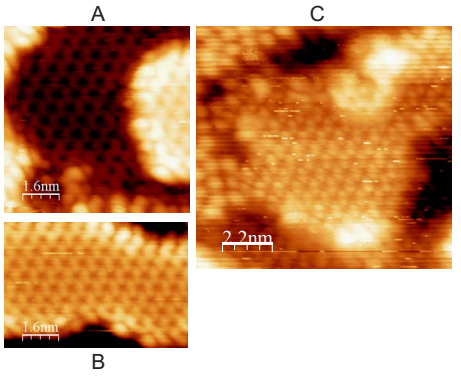

FIG. 6. (Color online) STM images showing the $\sqrt{3}$ structure in islands and holes, after preparation using different conditions. (a) and (b) Prepared by deposition at 500 K, followed by 10 min anneal. $V_T=-1.0$ V and $I_T=2$ nA. (c) Prepared by deposition at 600 K, followed by 2 min anneal. $V_T=-1.0$ V and $I_T=0.2$ nA.

increase in A_{island}. This can be rationalized, as described above, by the disappearance of small Ag-rich islands. In the same period, there is a steeper increase in A_{holes}, indicating that an additional factor contributes to hole expansion. Between 30 and 120 min, A_{hole} continues to increase, and this is compensated by a decrease in the area of the 7×7. The variation in A_{island} is much less than the other two variables. Throughout the experiment, but especially after the small islands have disappeared, the decrease in R_{IH} is predominantly due to an increase in its denominator, A_{hole}. In other words, the holes expand and consume the 7×7, while the islands do not change much in area. A reservoir of Ag must exist that feeds Ag into the holes during annealing, and correspondingly, a sink must exist that consumes the displaced Si without increasing the size of the $\sqrt{3}$ islands. We will propose that the edges of the $\sqrt{3}$ islands can serve as both.

B. Characteristics of the $\sqrt{3}$ in STM

Based upon the quality of the $\sqrt{3}$ in STM, two regimes can be identified (roughly): $R_{\text{IH}}\geq3$ and $3\geq R_{\text{IH}}\geq1$. The defining feature is the quality of the $\sqrt{3}$, which is much better in the second regime, $3\geq R_{\text{IH}}\geq1$. In the second regime, we observe many characteristics of the $\sqrt{3}$ that had been reported previously, including antiphase domains within the islands but not within the holes,[11] and occupation of different types of Si sites on the islands vs the holes.[9,11,30] High-resolution examples of the $\sqrt{3}$, prepared under different conditions, are shown in Fig. 6. The vertical separation between islands and holes, averaged over bias voltages between ±2 V and over 3 experiments where $3\geq R_{\text{IH}}\geq1$, is 0.293 ± 0.026 nm. This is compatible with 0.314 nm, which is the bulk separation between equivalent Si(111) planes, see Fig. 1(a).

In the same regime of R_{IH}, bright strips—rims—are often apparent at the edges of the $\sqrt{3}$ islands, as shown in Fig. 7 and in Fig. 6(b). The rims are usually in registry with the $\sqrt{3}$ on the island. This is particularly clear in Fig. 6(b). These rims are most pronounced when tunneling occurs into empty surface states (negative bias). These rims have been mentioned explicitly,[11] or shown in published data,[10] by other

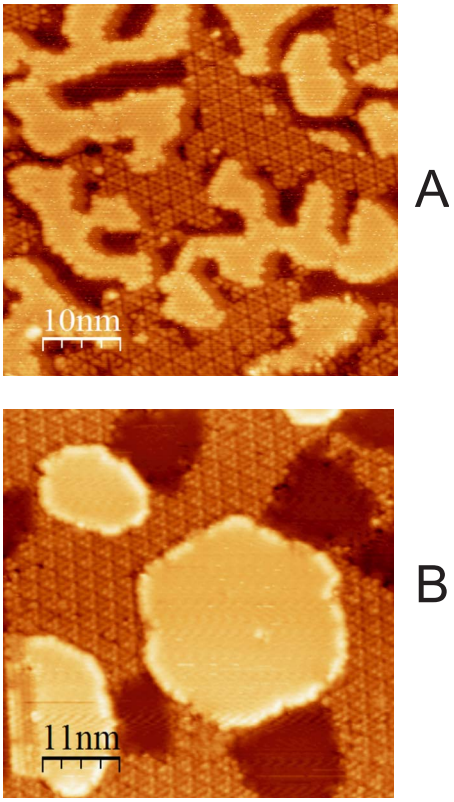

FIG. 7. (Color online) STM images of islands, showing rims. $V_T=-1.0$ V and $I_T=0.2$ nA. (a) Prepared by deposition at 615 K, annealed 2 min. 50×50 nm^2. (b) Prepared by deposition at 800 K, annealed 2 min. 65×65 nm^2.

authors as well. McComb, *et al.*[11] attributed them to strain. We hypothesize that they could be regions that are Ag-rich and Si-deficient, relative to the ideal $\sqrt{3}$ stoichiometry. Further discussion is deferred to Sec. IV.

In the other regime, where $R_{\text{IH}}\geq3$, the islands are rough and extended regions of $\sqrt{3}$ are rare. The holes typically show a much better $\sqrt{3}$ structure than the islands. It is reasonable to suppose that the islands have a Ag:Si ratio considerably higher than 1 because of their origin as Ag islands that nucleated at relatively low temperature.[6,7] Their far-from-complete conversion to $\sqrt{3}$ accounts for the high R_{IH} values, for instance, at $T_{\text{dep}}<600$ K in Fig. 3.

C. Computational results

Another explanation for the data could involve different types of $\sqrt{3}$ structures—perhaps including metastable phase(s) with high Ag:Si ratios. We tested this possibility with a GA search for different types of $\sqrt{3}$ structures. The result is given in Fig. 8. In order to show the variation in both Si and Ag coverage, a two-digit notation is used for the x axis. The first digit is the number of Si atoms and the second digit is the number of Ag atoms. In the bottom x-axis labels, these numbers are normalized to the (1×1) unit-cell area, and in the top axis they are normalized to the $\sqrt{3}$ unit-cell area. The point with the lowest E_f has $x=(1,1)$ per (1×1). This is the IET structure. The energy of the (7×7) is

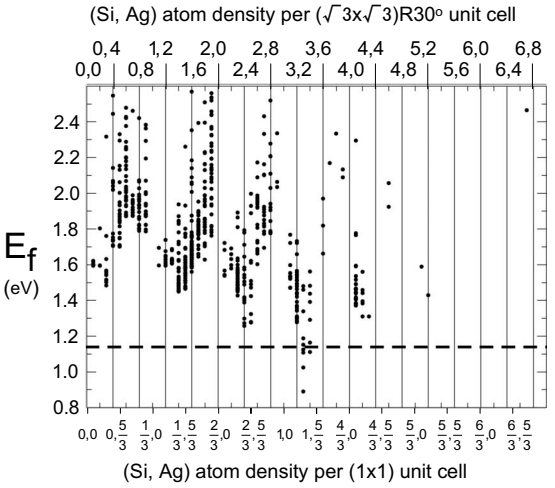

FIG. 8. Genetic algorithm search results, showing E_f for various $\sqrt{3}$ structures. Each value of the abscissa is labeled with both the Si coverage (first digit) and the Ag coverage (second digit) on the bottom axis, equivalent to $N_{\sqrt{3},Si}$ and $N_{\sqrt{3},Ag}$. For each value of $N_{\sqrt{3},Si}$ (first digit), the value of $N_{\sqrt{3},Ag}$ ranges from 0 to 3. The (7×7) energy is the dashed horizontal line. The top axis is labeled with the number of Si and Ag atoms per $\sqrt{3}$ unit cell, i.e., each value on the lower axis is multiplied by 3.

shown by the dashed horizontal line. [The surface energy of (2×1) Si(111) is calculated with DFT, and the (7×7) Si(111) is taken to be 0.33 eV/(1×1) lower than the (2×1) surface.[15]] We conclude that the IET is the only $\sqrt{3}$ structure that is more stable than the (7×7), and hence is the only viable model for the portions of the surface identified experimentally as $\sqrt{3}$.

IV. DISCUSSION

This work shows that values of R_{IH} up to 3 can be obtained even when the islands and holes all show a reasonably good $\sqrt{3}$ structure. A GA search using DFT shows that the high values of R_{IH} cannot be due to the existence of different, perhaps metastable, forms of the $\sqrt{3}$. Instead, we propose that it is due to deviation from stoichiometry at the rims of the $\sqrt{3}$ islands. Specifically, we propose that the rims are Ag rich. Under conditions where the islands become more compact, the rims release Ag, which triggers growth of the holes. The Ag from the islands is replaced by Si from the (growing) holes, causing no net change in island area.

Ueno *et al.*[31] previously proposed that edges of $\sqrt{3}$ islands and terraces serve as reservoirs for a two-dimensional gas of Ag adatoms on top of the $\sqrt{3}$, and that local variation in the density of the gas causes broadening in photoemission spectra of Si. They based this upon their observation that spectral narrowing correlates with faceting of the $\sqrt{3}$ island edges and conversion to a 6×1 structure at the islands' edges (at high temperature, 875 K). Our model draws upon, and supports, their conclusion about the role of $\sqrt{3}$ island edges.

In our model, Ag and Si must both diffuse across the $\sqrt{3}$ hole in order for it to expand at the border with (7×7). This is illustrated schematically in Fig. 9, where the $\sqrt{3}$ hole is

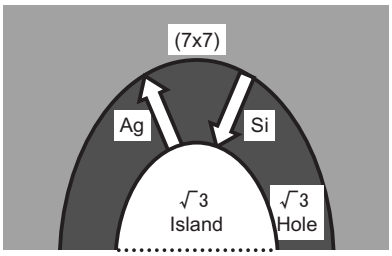

FIG. 9. Schematic illustration of the growth of a hole around a $\sqrt{3}$ island.

drawn as a "moat" surrounding the $\sqrt{3}$ island because this configuration is often seen in the data. [See Figs. 3(a)–3(d).] Diffusion of both Si and Ag on the $\sqrt{3}$ is expected to be facile. For Si, Minami *et al.*[32] report that the diffusion coefficient of Si is higher on the $\sqrt{3}$ than on the (7×7) by a factor of 60. For Ag, Nakajima *et al.*[33,34] have established that a two-dimensional gas of Ag adatoms exists on the $\sqrt{3}$ at room temperature. This implies high mobility. Furthermore, STM observations show that Ag atoms on the $\sqrt{3}$ become mobile, on the time scale of STM scanning, already between 6 and 60 K.[35] In comparison, long-range diffusion of Ag atoms on the (7×7) is much slower. For instance, at room temperature, a single Ag atom moves easily within a half unit cell of the (7×7) but it hops between these units at a rate of only 10^{-5} s^{-1}.[36–38] Thus, it is plausible to surmise that Ag released from the $\sqrt{3}$ island, and Si released from the $\sqrt{3}$ hole, can quickly find sites for incorporation within the local $\sqrt{3}$ area and do not move out into the (7×7).

We can now explain—at least partially—the observations of McComb *et al.*[11] introduced in Sec. I. They found that $R_{IH}>1$, at three out of four Ag coverages measured.[11] Their $T_{dep}=720$ K was too low to achieve the limiting value of R_{IH}. In fact, from their data R_{IH} varied from about 1.8 to 1.2, at 0.4–0.8 ML of Ag. This is compatible with the value of 1.7 shown in Fig. 3, at 0.7 ML and at $T_{dep}=700$ K.

Finally, note that there is a dramatic change in island shape and island size, between T_{dep} of 600 and 700 K, in Fig. 3. At 600 K, the islands are much smaller and more ramified. This reflects the kinetics of nucleation, as well as limited island reshaping and coarsening. This may be related to an observation by Raynerd, *et al.*,[17,18] who showed that there is a strong increase in the measured surface concentration of Ag, between 600 and 700 K, after a fixed Ag exposure sufficient to saturate the surface with $\sqrt{3}$. We speculate that Ag at the island rims may not be directly at the surface. If it is slightly buried, then the *apparent* surface concentration of Ag could increase as the islands become larger and more compact. Previously, Denier van der Gon and Tromp[16] proposed that the increase in apparent Ag coverage is due to a decrease in the occurrence of antiphase boundaries in the $\sqrt{3}$, where Ag density is low. We suggest that participation of $\sqrt{3}$ island edges may be an additional factor.

V. CONCLUSIONS

Using STM, we have shown that values of R_{IH} as high as 3 can be obtained under conditions where both islands and

holes are covered by the $\sqrt{3}$ phase. However, the limiting value of R_{IH} is 1. This value is achieved by deposition at 800 K, and it can be approached by annealing at lower temperatures. A genetic algorithm DFT search does not reveal any $\sqrt{3}$ phase that could be energetically competitive with the IET structure. We propose that values of R_{IH} between about 3 and 1 are due, at least partly, to the presence of excess Ag at edges of ramified $\sqrt{3}$ islands. Under certain conditions, the higher values can also be attributed to the existence of small islands that are Ag rich.

ACKNOWLEDGMENTS

This work was supported by the U.S. Department of Energy, Office of Basic Energy Science, Division of Materials Sciences and Engineering. The research was performed at the Ames Laboratory. Ames Laboratory is operated for the U.S. Department of Energy by Iowa State University under Contract No. DE-AC02-07CH11358.

APPENDIX

If both islands and holes are covered with perfect $\sqrt{3}$ phase, the density of Si in the $\sqrt{3}$ is related to R_{IH} by[9–11]

$$N_{Si,\sqrt{3}} = N_{Si,7} - \frac{2A_{island}}{A_{island} + A_{hole}} = N_{Si,7} - \frac{2R_{IH}}{1 + R_{IH}}. \quad \text{(A1)}$$

Here, A is area of the type of $\sqrt{3}$ indicated by the subscript [normalized to the (1×1) unit cell area], and N_{Si} is the number of Si atoms in the structure indicated by the subscript [i.e., ($\sqrt{3}$ or (7×7)], within the area of a (1×1) unit cell. The factor of $2A_{island}$ appears because islands are higher than holes by a bilayer of Si. See Fig. 1(a). Since it is known that $N_{Si,7}=2.08$ (vs 2.00 for the unreconstructed surface),[39] experimental measurement of R_{IH} yields $N_{Si,\sqrt{3}}$ from Eq. (A1). If $N_{Si,\sqrt{3}}=1.00$ as in the IET model, then ideally $R_{IH}=53/45 \approx 1.18$ from exact mass balance. In the text, for simplicity, the ideal value of R is given as 1. To relate surface atom densities, N, to notation used in the main text, note that $N_{Si,\sqrt{3}}=1.00$ or $N_{Ag,\sqrt{3}}=1.00$ is equivalent to 1 ML of Si or Ag, respectively.

*Present address: Department of Chemical Engineering, Massachusetts Institute of Technology, Cambridge, MA 02139, USA.

[1] H. P. Bonzel and S. Ferrer, Surf. Sci. **118**, L263 (1982).
[2] J. C. Campuzano, A. M. Lahee, and G. Jennings, Surf. Sci. **152-153**, 68 (1985).
[3] T. Gritsch, D. Coulman, R. J. Behm, and G. Ertl, Phys. Rev. Lett. **63**, 1086 (1989).
[4] A. Klust and R. J. Madix, J. Chem. Phys. **126**, 084707 (2007).
[5] V. G. Lifshits, A. A. Saranin, and A. V. Zotov, *Surface Phases on Silicon: Preparation, Structures, and Properties* (Wiley, West Sussex, England, 1994).
[6] A. Shibata, Y. Kimura, and K. Takayanagi, Surf. Sci. **303**, 161 (1994).
[7] A. Shibata, H. Kimura, and K. Takayanagi, J. Vac. Sci. Technol. B **12**, 2026 (1994).
[8] A. Shibata and K. Takayanagi, Jpn. J. Appl. Phys. **32**, 1385 (1993).
[9] A. Shibata, Y. Kimura, and K. Takayanagi, Surf. Sci. **275**, L697 (1992).
[10] K. J. Wan, X. F. Lin, and J. Nogami, Phys. Rev. B **47**, 13700 (1993).
[11] D. W. McComb, D. J. Moffatt, P. A. Hackett, B. R. Williams, and B. F. Mason, Phys. Rev. B **49**, 17139 (1994).
[12] I. Mochizuki, R. Negishi, and Y. Shigeta, J. Phys.: Conf. Ser. **61**, 1056 (2007).
[13] H. Aizawa, M. Tsukada, N. Sato, and S. Hasegawa, Surf. Sci. **429**, L509 (1999).
[14] N. Sato, T. Nagao, and S. Hasegawa, Surf. Sci. **442**, 65 (1999).
[15] Y. G. Ding, C. T. Chan, and K. M. Ho, Phys. Rev. Lett. **67**, 1454 (1991).
[16] A. W. Denier van der Gon and R. M. Tromp, Phys. Rev. Lett. **69**, 3519 (1992).
[17] G. Raynerd, T. N. Doust, and J. A. Venables, Surf. Sci. **261**, 251 (1992).
[18] G. Raynerd, M. Hardiman, and J. A. Venables, Phys. Rev. B **44**, 13803 (1991).
[19] B. Unal, F. Qin, Y. Han, D. J. Liu, D. Jing, A. R. Layson, C. J. Jenks, J. W. Evans, and P. A. Thiel, Phys. Rev. B **76**, 195410 (2007).
[20] I. Horcas, R. Fernandez, J. M. Gomez-Rodriguez, J. Colchero, J. Gomez-Herrero, and A. M. Baro, Rev. Sci. Instrum. **78**, 013705 (2007).
[21] K. Sakamoto, T. Suzuki, K. Mawatari, K. Kobayashi, J. Okabayashi, K. Ono, N. Ueno, and M. Oshima, Phys. Rev. B **73**, 193303 (2006).
[22] I. Matsuda, H. Morikawa, C. Liu, S. Ohuchi, S. Hasegawa, T. Okuda, T. Kinoshita, C. Ottaviani, A. Cricenti, M. D'angelo, P. Soukiassian, and G. Le Lay, Phys. Rev. B **68**, 085407 (2003).
[23] Y. Nakamura, Y. Kondo, J. Nakamura, and S. Watanabe, Phys. Rev. Lett. **87**, 156102 (2001).
[24] H. M. Zhang, J. B. Gustafsson, and L. S. O. Johansson, J. Phys.: Conf. Ser. **61**, 1336 (2007).
[25] H. M. Zhang, J. B. Gustafsson, and L. S. O. Johansson, Phys. Rev. B **74**, 201304(R) (2006).
[26] W. Kohn and L. J. Sham, Phys. Rev. **140**, A1133 (1965).
[27] P. Hohenberg and W. Kohn, Phys. Rev. **136**, B864 (1964).
[28] G. Kresse and D. Joubert, Phys. Rev. B **59**, 1758 (1999).
[29] G. Kresse and J. Hafner, Phys. Rev. B **47**, 558 (1993).
[30] K. J. Wan, X. F. Lin, and J. Nogami, Phys. Rev. B **45**, 9509 (1992).
[31] M. Ueno, I. Matsuda, C. Liu, and S. Hasegawa, Jpn. J. Appl. Phys. **42**, 4894 (2003).
[32] T. Minami, T. Hashizume, and A. Ichimiya, e-J. Surf. Sci. Nanotechnol. **7**, 763 (2009).
[33] Y. Nakajima, S. Takeda, T. Nagao, S. Hasegawa, and X. Tong, Phys. Rev. B **56**, 6782 (1997).
[34] Y. Nakajima, G. Uchida, T. Nagao, and S. Hasegawa, Phys. Rev. B **54**, 14134 (1996).

[35] N. Sato, T. Nagao, and S. Hasegawa, Phys. Rev. B **60**, 16083 (1999).
[36] T. Jarolímek, J. Mysliveček, P. Sobotík, and I. Ošt'ádal, Surf. Sci. **482-485**, 386 (2001).
[37] P. Sobotík, P. Kocán, and I. Ošt'ádal, Surf. Sci. **537**, L442 (2003).
[38] C. Zhang, G. Chen, K. Wang, H. Yang, T. Su, C. T. Chan, M. M. T. Loy, and X. Xiao, Phys. Rev. Lett. **94**, 176104 (2005).
[39] K. Oura, V. G. Lifshits, A. A. Saranin, A. V. Zotov, and M. Katayama, *Surface Science: An Introduction* (Springer, Berlin, 2003).